## Ch. 7 Wavelets and Multiresolution Processing

Wavelet based transformations from a multiresolution point of view :

Preview

- What is multi-resolution?
- The difference between Fourier transform and Wavelet transform

Background

- Both small and large objects, or low and high contrast objects are present
- Examine an object --Depending on the size or contrast of the object
- Local histogram variations (Fig. 7.1)

## Fourier / Wavelet transformatoin

Basis function

- Sinusoids / wavelets (varying frequency and limited duration)
- A musical score for an image

Multiresolution Theory

- Representation and analysis of signals (or images) at more than one resolution.
- features that might go undetected at one resolution may be easy to spot at another.
  - Subband coding
  - Quadrature mirror filtering
  - Pyramidal image processing

## Background

If the objects are small in size or low in contrast → examine them at high resolutions;
If they are large in size or high in contrast → a coarse view is all that is required.
If both small and large objects-or low and high contrast objects-are present simultaneously, it can be advantageous to study them at several resolutions

FIGURE 7.1 A natural image and its local histogram variations.

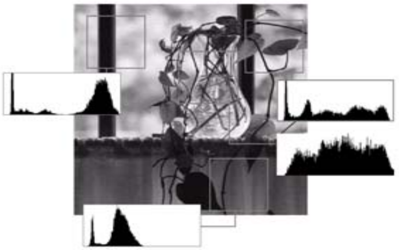

## Image Pyramids

A powerful, but conceptually simple structure for representing images at more than one resolution

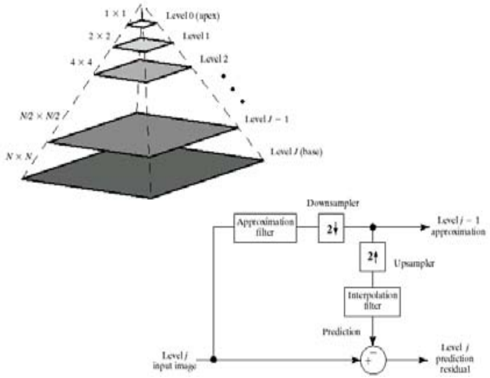


a b

FIGURE 7.2 (a) A pyramidal image structure and (b) system block diagram for creating it.

## Image Pyramids

Image Pyramids

- What is an image pyramid?
- Block diagram for image pyramid
  - Approximation pyramid
  - Prediction pyramid

Matrix pyramids

- A sequence of images are used when it is necessary to work with image at different resolutions simultaneously

Tree pyramids

- use several resolutions simultaneously

## Image Pyramids

Quad-trees

- Modifications of T-pyramids
- Every node of the tree except the leaves has four children
- The image is divided into four quadrants at each hierarchical level
- If a parent node has four children if the same value, it is not necessary to record them

Matrix pyramids

- The total number of elements in a P+1 level pyramid
- Approximation pyramid
- Prediction residual pyramid
- An image with level J and its P reduced resolution
  - Contains a low-resolution approximation of the original at level J-P and information for the construction of P higher-resolution approximation at the other level

## Image Pyramids

Step 1: filtering and down-sampling

Mean pyramid(mean),
Gaussian pyramid(low-pass Gaussian filter),
sub-sampling pyramid(no filtering )

Step 2 : up-sample by a factor of 2.

Create a prediction image
Determines how accurately approximate the input by using interpolation
If we delete interpolation filter, blocky effect is inevitable

## Image Pyramids

Step3 : compute the difference between the prediction of step2 and the input to step 1 (prediction residual)

Predict residual of level J

Coarse to fine strategy

High resolution pyramid—used for analysis of large structure or overall image context

Low resolution pyramid —analyzing individual object characteristics

## Image Pyramids

Prediction residual--Laplacian pyramid

- ✓64x64 Laplacian pyramid predict the Gaussian pyramid's level 7 prediction residual
- ✓First order statistics of the pyramid are highly peaked around zero

## Image Pyramids

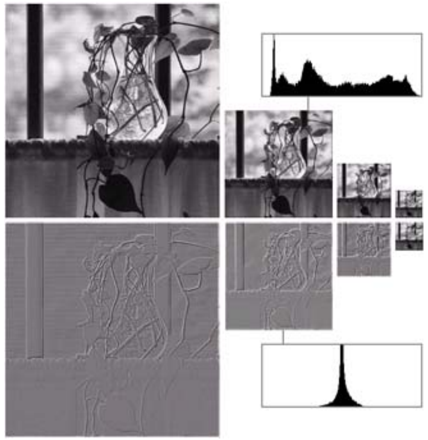

a
b
**FIGURE 7.3** Two image pyramids and their statistics: (a) a Gaussian (approximation) pyramid and (b) a Laplacian (prediction residual) pyramid.

## Subband coding

a
b
**FIGURE 7.4** (a) A two-band filter bank for one-dimensional subband coding and decoding, and (b) its spectrum splitting properties.

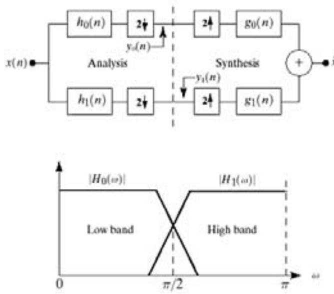


## Sub-band coding

- An image is decomposed into a set of band-limited component sub-bands, which can be reassemble to reconstruct the original image
- The output sequence is formed through the decomposition of $x(n)$ into $y_0(n)$ and $y_1(n)$ via analysis filter $h_0(n)$ and $h_1(n)$,and subsequent recombination via synthesis filters $g_0(n)$ and $g_1(n)$

| Filter | QMF | CQF | Orthonormal |
|---|---|---|---|
| $H_0(z)$ | $H_0^2(z) - H_0^2(-z) = 2$ | $H_0(z)H_0(z^{-1}) +$ $H_0^2(-z)H_0(-z^{-1}) = 2$ | $G_0(z^{-1})$ |
| $H_1(z)$ | $H_0(-z)$ | $z^{-1}H_0(-z^{-1})$ | $G_1(z^{-1})$ |
| $G_0(z)$ | $H_0(z)$ | $H_0(z^{-1})$ | $G_0(z)G_0(z^{-1}) +$ $G_0(-z)G_0(-z^{-1}) = 2$ |
| $G_1(z)$ | $-H_0(-z)$ | $zH_0(-z)$ | $-z^{-2K+1}G_0(-z^{-1})$ |

**TABLE 7.1** Perfect reconstruction filter families.

## Sub-band coding

- Bio-orthogonal- filter bank satisfying the conditions
- Filter response of two-band, real coefficient, perfect reconstruction filter bank are subject to bio-orthogonality constraints
- Orthonormal
- Two-dimensional four-band filter bank for subband image coding (with one-dimensional filter in Table1)

## Impulse responses

FIGURE 7.6 The impulse responses of four 8-tap Daubechies orthonormal filters.

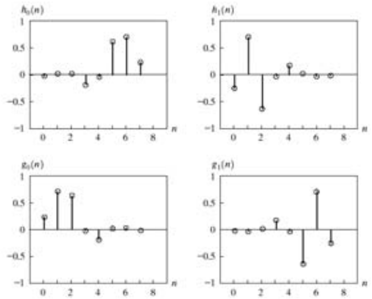


## 4 band split

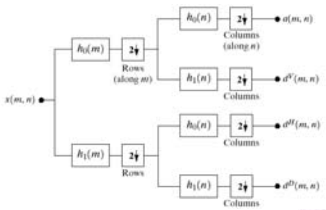


FIGURE 7.5 A two-dimensional, four-band filter bank for subband image coding.

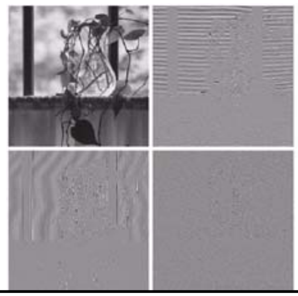

FIGURE 7.7 A four-band split of the vase in Fig. 7.1 using the subband coding system of Fig. 7.5.

## The Harr transform

Its *basis functions* are the oldest and simplest known *orthonormal* wavelets.

Separable, symmetric, can be expressed in matrix form
**T=HFH**

The *Harr basis functions* $h_k(z)$ are

$$h_0(z) = h_{00}(z) = \sqrt{\frac{1}{N}}, \ z \in [0,1]$$

*and*

$$h_k(z) = h_{pq}(z) = \sqrt{\frac{1}{N}} \begin{cases} 2^{p/2} & (q-1)/2^p \le z < (q-0.5)/2^p \\ -2^{p/2} & (q-0.5)/2^p \le z < q)/2^p \\ 0 & otherwise \end{cases}, \ z \in [0,1]$$

Discrete wavelet transform using *Harr basis functions*

## The Harr transform

$$\mathbf{H}_4 = \frac{1}{\sqrt{4}}\begin{bmatrix} 1 & 1 & 1 & 1 \\ 1 & 1 & -1 & -1 \\ \sqrt{2} & -\sqrt{2} & 0 & 0 \\ 0 & 0 & \sqrt{2} & -\sqrt{2} \end{bmatrix}$$

$$\mathbf{H}_2 = \frac{1}{\sqrt{2}}\begin{bmatrix} 1 & 1 \\ 1 & -1 \end{bmatrix}$$

## The Harr transform

1. Its local statistics are relatively constant and easily modeled.
2. Many of its values are close to zero → image compression.
3. Both coarse and fine resolution approximations of the original image can be extracted.

Figures 7.8(b)-(d) were reconstructed from the subimages of Fig. 7.8(a).

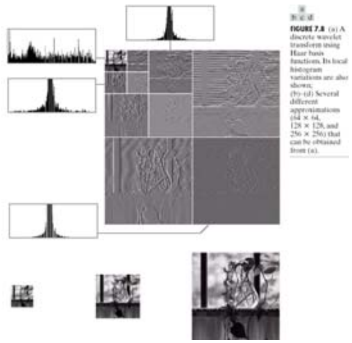

## Laplacian pyramid, subband coding and the Harr transform

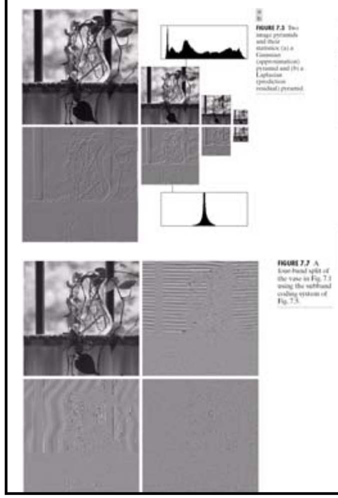

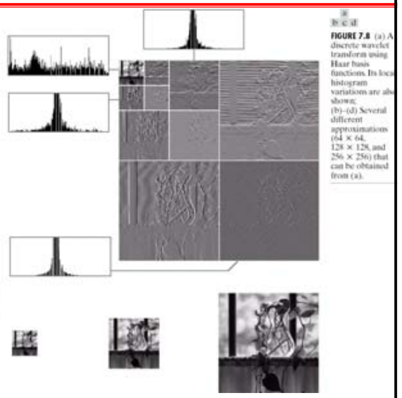

## Multiresolution Expansions

***Scaling functions*** : create a series of approximations

***Wavelets*** : encode the difference of adjacent approximations

Series expansions

- A signal $f(x)$ : a linear combination of expansion functions

$$f(x) = \sum_k \alpha_k \varphi_k(x)$$

  - Expansion coefficients $\alpha_k$
  - Expansion functions $\varphi_k(x)$
  - If the expansion is unique, expansion functions are called *basis functions*
  - Expansion set $\{\varphi_k(x)\}$ is called a *basis* for the functions
- *Closed span* of the expansion set, denoted $V = \overline{\underset{k}{Span}\{\varphi_k(x)\}}$

## Multiresolution Expansions

- ***Dual functions*** $\{\tilde{\varphi}_k(x)\}$ for $\{\varphi_k(x)\}$
- ***Integral inner products***

$$\alpha_k = \langle \tilde{\varphi}_k(x), f(x) \rangle = \int \tilde{\varphi}_k^*(x) f(x) dx$$

- Three cases using vectors in two-dimensional Euclidean space
  1. If expansion functions are orthonormal basis for $V$, or

$$\langle \varphi_j(x), \varphi_k(x) \rangle = \delta_{jk} = \begin{cases} 0 & j \neq k \\ 1 & j = k \end{cases}$$

$$\varphi_k(x) = \tilde{\varphi}_k(x)$$

$$\alpha_k = \langle \tilde{\varphi}_k(x), f(x) \rangle = \langle \varphi_k(x), f(x) \rangle$$

  2. If orthogonal, $\langle \varphi_j(x), \varphi_k(x) \rangle = \delta_{jk} = 0 \quad j \neq k$

$$\langle \varphi_j(x), \tilde{\varphi}_k(x) \rangle = \delta_{jk} = \begin{cases} 0 & j \neq k \\ 1 & j = k \end{cases}$$

*biorthogonal*

  3. If the expansion set is not a basis for $V$, but supports the expansion, it is a spanning set, with non-unique expansion coefficients – expansion functions and their duals are overcomplete or redundant

## Case 3 of Multiresolution Expansions

- If the expansion set is not a basis for $V$, but supports the expansion, it is a spanning set, with non-unique expansion coefficients – expansion functions and their duals are *overcomplete* or *redundant*
- They form a frame in which

$$A\|f(x)\|^2 \leq \sum_k |\langle \varphi_k(x), f(x) \rangle|^2 \leq B\|f(x)\|^2$$

$$A \leq \frac{\sum_k |\langle \varphi_k(x), f(x) \rangle|^2}{\|f(x)\|^2} \leq B$$

, for some A and B.

- A and B "*frame*" the normalized inner products of the expansion coefficients and the function.
- If A=B, the expansion set is called a tight frame and it can be shown that

$$f(x) = \frac{1}{A} \sum_k \langle \varphi_k(x), f(x) \rangle \varphi_k(x)$$

## Scaling functions

Scaling functions —the shape of $\varphi(x)$ changes with $j$

- Expansion functions composes of integer translation and binary scaling of the *real, square-integrable function* $\varphi(x)$;

$$\varphi_{j,k}(x) = 2^{j/2} \varphi(2^j x - k)$$

  - $k$ : position, $j$: width, height?
- By choosing $\varphi(x)$ wisely, $\{\varphi_{j,k}(x)\}$ can be made to span $L^2(\mathbf{R})$
- If $j = j_0$ , then $\{\varphi_{j0,k}(x)\}$ is a subset of $\{\varphi_{j,k}(x)\}$, creating a subspace $V_j$
- Increasing j increases Vj, allowing functions with smaller variations or finer detail to be in the subspace.

## The Harr scaling functions

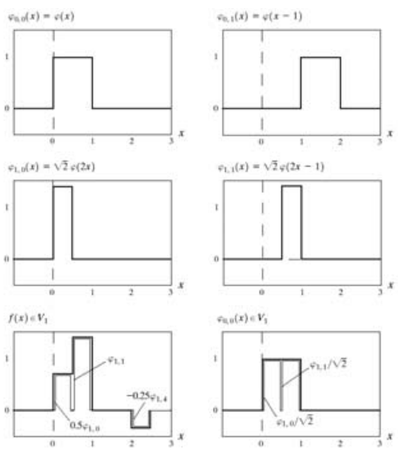

a b
c d
e f

**FIGURE 7.9** Haar scaling functions in $V_0$ in $V_1$.

## The Harr transform

FIGURE 7.10 The nested function spaces spanned by a scaling function.

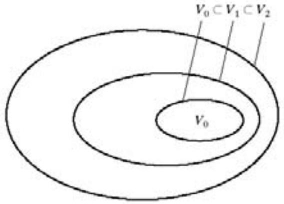


## MRA requirements

1. The scaling function is *orthogonal* to its integer translates.
2. The subspaces spanned by the scaling function at low scales are nested within those spanned at higher scales
3. The only function that is common to all $V_j$, is $f(x) = 0$, or

$$V_{-\infty} = \{0\}$$

4. Any function can be represented with arbitrary precision, or

$$V_{\infty} = \{L^2(\mathbf{R})\}$$

## MRA equation

$$\varphi(x) = \sum_n h_\varphi(n)\sqrt{2}\varphi(2x-n)$$

Refinement equation, MRA equation, dilation equation

- The expansion functions of any subspace can be built from double resolution copies of themselves
- Scaling function coefficients : $h_\varphi(n)$
- Scaling vector : $h_\varphi$

## Wavelet functions

- Given a scaling function that meets the MRA requirements of the previous section,
- we can define a wavelet function $\psi(x)$ that, together with its integer translates and binary scalings, spans the difference between any two adjacent scaling subspaces, $V_j$ and $V_{j+1}$

$$\psi_{j,k}(x) = 2^{j/2}\psi(2^j x - k)$$

## Wavelet functions

A wavelet function $\psi(x)$

- Spans the difference between $V_j$ and $V_{j+1}$

$$W_j = \overline{Span_k\{\psi_{j,k}(x)\}} \qquad V_{j+1} = V_j \oplus W_j$$

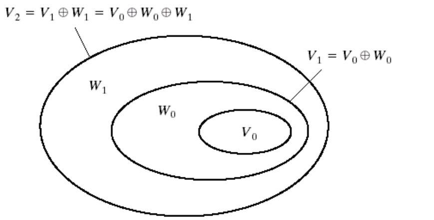


**FIGURE 7.11** The relationship between scaling and wavelet function spaces.

## Wavelet equation in double resolution functions

$$\psi(x) = \sum_n h_\psi(n)\sqrt{2}\psi(2x-n)$$

Refinement equation, MRA equation, dilation equation

- The expansion functions of any subspace can be built from double resolution copies of themselves
- wavelet function coefficients : $h_\psi(n)$
- wavelet vector : $h_\psi$

$$W_j = \overline{Span_k\{\psi_{j,k}(x)\}}$$

## The Harr wavelet functions

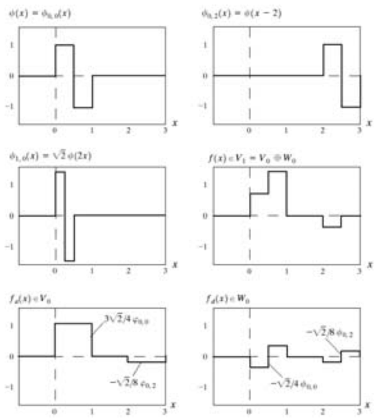

a b
c d
e f

**FIGURE 7.12** Haar wavelet functions in $W_0$ and $W_1$.

## Wavelet Transformations

- Generalized wavelet series expansion
- Discrete wavelet transform
- Continuous wavelet transform.

*Fourier* counterparts?

## Wavelet Series Expansion

$$f(x)=\sum_k c_{j_0}(k)\varphi_{j_0,k}(x)+\sum_{j=j_0}^{\infty}\sum_k d_j(k)\psi_{j,k}(x)$$

- Approximation or scaling coefficients : $c_{j0}(k)$
- Detail or wavelet coefficients : $d_j(k)$

## Harr wavelet expansion

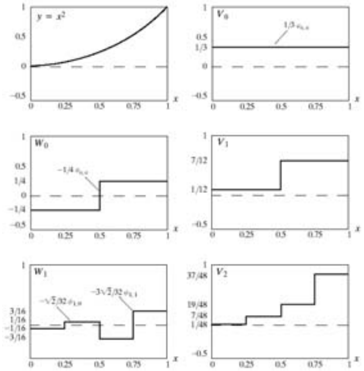

a b
c d
e f

FIGURE 7.13 A wavelet series expansion of $y = x^2$ using Haar wavelets.

## Discrete Wavelet Transform

Wavelet series expansion : a function → a sequence of coeffiecients

$$f(x)=\sum_k c_{j_0}(k)\varphi_{j_0,k}(x)+\sum_{j=j_0}^{\infty}\sum_k d_j(k)\psi_{j,k}(x)$$

DWT : if the function is a sequence of numbers, the resulting coefficients are called DWT of $f(x)$

: Approximation and detail coefficients

$$W_\varphi(j_0,k)=\frac{1}{\sqrt{M}}\sum_x f(x)\varphi_{j_0,k}(x)$$

$$W_\psi(j,k)=\frac{1}{\sqrt{M}}\sum_x f(x)\psi_{j,k}(x)$$

$$f(x)=\frac{1}{\sqrt{M}}\sum_k W_\varphi(j_0,k)\varphi_{j_0,k}(x)+\frac{1}{\sqrt{M}}\sum_{j=j_0}^{\infty}\sum_k W_\psi(j,k)\psi_{j,k}(x)$$

* normalizing factor : $\frac{1}{\sqrt{M}}$

## Continuous Wavelet Transform

A continuous function → a highly redundant function of two continuous variables – translation and scale.

CWT :

$$W_\psi(s,\tau)=\int_{-\infty}^{\infty} f(x)\psi_{s,\tau}(x)dx$$

$$\psi_{s,\tau}(x)=\frac{1}{\sqrt{s}}\psi\left(\frac{x-\tau}{s}\right)$$

Inverse CWT :

$$f(x)=\frac{1}{C_\psi}\int_0^{\infty}\int_{-\infty}^{\infty} W_\psi(s,\tau)\frac{\psi_{s,\tau}(x)}{s^2}d\tau ds$$

$$C_\psi=\int_{-\infty}^{\infty}\frac{|\Psi(u)|^2}{|u|}du$$

* normalizing factor : $\frac{1}{\sqrt{M}}$

## Continuous Wavelet transform

a b
c d

FIGURE 7.14 The continuous wavelet transform (c and d) and Fourier spectrum (b) of a continuous one-dimensional function (a).

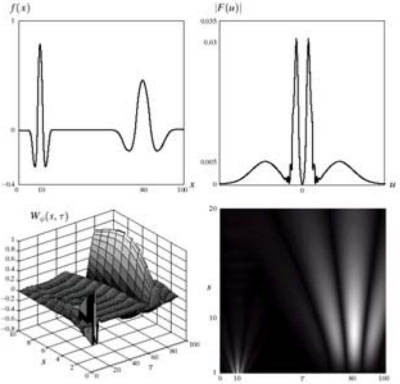

## Fast Wavelet Transform: Mallat's Herringbone algorithm

Exploits a surprising but fortunate relationship between the coefficients of the DWT at adjacent scales.

FIGURE 7.15 An FWT analysis bank.

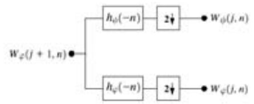

## Fast Wavelet Transform

Multiresolution refinement equation : $\varphi(x)=\sum_n h_\varphi(n)\sqrt{2}\varphi(2x-n)$

Scaling $x$ by $2^j$, translating by $k$, and let $m=2k+n$:

$$\varphi(2^j x-k)=\sum_n h_\varphi(n)\sqrt{2}\varphi(2(2^j x-k)-n)$$
$$=\sum_m h_\varphi(m-2k)\sqrt{2}\varphi(2^{j+1} x-m)$$

Similarly, $\psi(2^j x-k)=\sum_m h_\psi(m-2k)\sqrt{2}\varphi(2^{j+1} x-m)$

Wavelet (detail) coefficient : $W_\psi(j,k)=\sum_m h_\psi(m-2k)W_\varphi(j+1,m)$

$$W_\varphi(j,k)=\sum_m h_\varphi(m-2k)W_\varphi(j+1,m)$$

Detail and approximation coefficients of scale j are a function of approximation coefficients at scale j+1.

## Fast Wavelet Transform

$$W_\psi(j,k)=h_\psi(-n)*W_\varphi(j+1,n)$$
$$W_\varphi(j,k)=h_\varphi(-n)*W_\varphi(j+1,n), n=2k, k\geq 0$$

Scale j approximation and detail coefficients can be computed by convolving $W_\varphi(j+1, k)$ , the scale j + 1 approximation coefficients, with the time-reversed scaling and wavelet vectors, $h_\varphi(-n)$ and $h_\psi(-n)$, and subsampling the results.

Evaluating convolutions at nonnegative, even indices is equivalent to filtering and downsampling by 2.

FIGURE 7.15 An FWT analysis bank.

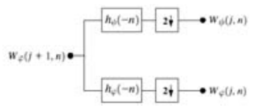

## 2-stage FWT

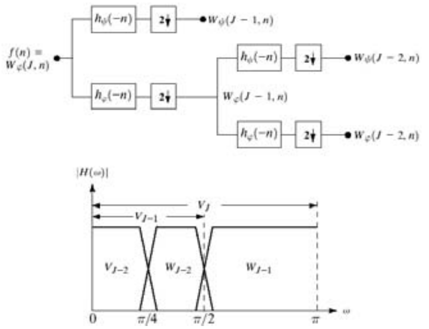

FIGURE 7.16 (a) A two-stage or two-scale FWT analysis bank and (b) its frequency splitting characteristics.

## FWT of f(n) = {1, 4, -3, 0}

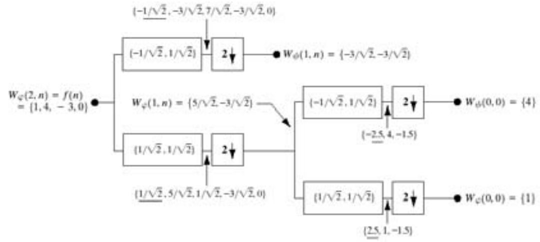

FIGURE 7.17 Computing a two-scale fast wavelet transform of sequence {1, 4, −3, 0} using Haar scaling and wavelet vectors.

## Inverse FWT

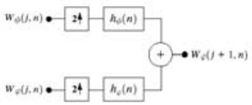

FIGURE 7.18 The $FWT^{-1}$ synthesis filter bank.

FIGURE 7.19 A two-stage or two-scale $FWT^{-1}$ synthesis bank.

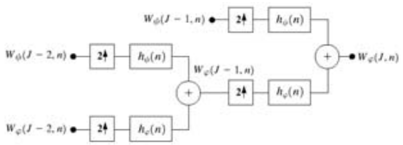

## Inverse FWT

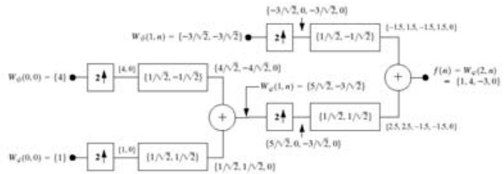

FIGURE 7.20 Computing a two-scale inverse fast wavelet transform of sequence $\{1, 4, -1.5\sqrt{2}, -1.5\sqrt{2}\}$ with Haar scaling and wavelet vectors.

## FFT vs. FWT

1. Computation complexity of FWT : O(M) of a length M sequence, while FFT algorithm requires O(M log M).
2. Transforms' basis functions.
   - Fourier basis functions (i.e., sinusoids) guarantee the existence of the FFT
   - The existence of the FWT depends upon the availability of a scaling function for the wavelets being used, as well as the orthogonality (or biorthogonality) of the scaling function and corresponding wavelets.
   - Mexican hat wavelet of Eq. (7.3-12), which does not have a companion scaling function, cannot be used in the computation of the FWT.
3. Finally, we note that while time and frequency are usually viewed as different domains when representing functions, they are inextricably linked.
   - *Heisenberg* uncertainty principle : If you want precise information about time, you must put up with some vagueness about frequency, and vice versa.
   - The tile in a time-frequency plane, also called a Heisenberg cell or Heisenberg box, shows where the basis function's energy is concentrated. Basis functions that are orthonormal are characterized by nonoverlapping tiles.

## Time-frequency tiling

- The time and frequency resolution of the FWT tiles vary, but the area of each tile is the same.
- That is, each tile represents an equal portion of the time-frequency plane.
- At low frequencies, the tiles are shorter (i.e., have better frequency resolution or less ambiguity regarding frequency) but are wider (which corresponds to poorer time resolution or more ambiguity regarding time).
- At high frequencies, tile width is smaller (so the time resolution is improved) and tile height is greater (which means the frequency resolution is poorer).

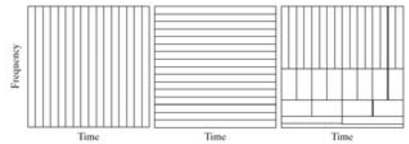


a b c
**FIGURE 7.21** Time-frequency tilings for (a) sampled data, (b) FFT, and (c) FWT basis functions.

## 2D Fast Wavelet Transform

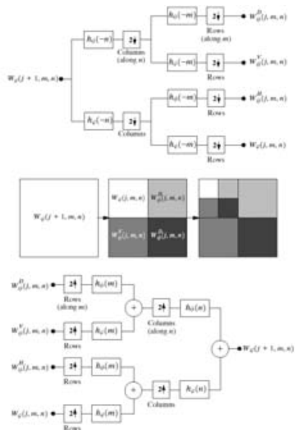

a b c
**FIGURE 7.22** The two-dimensional fast wavelet transform: (a) the analysis filter bank; (b) the resulting decomposition; and (c) the synthesis filter bank.

## 2D Fast Wavelet Transform

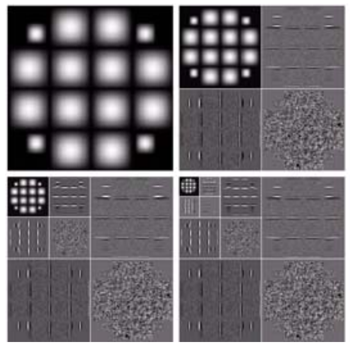

a b
c d
**FIGURE 7.23** A three-scale FWT.

## Symlets(symmetrical wavelets)

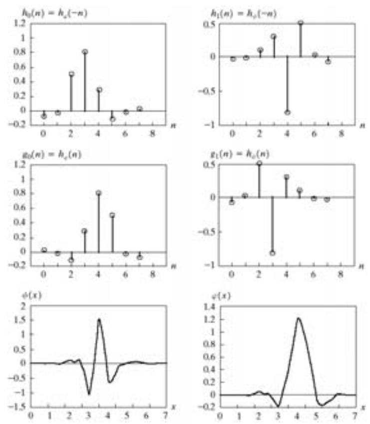

a b
c d
e f
g

**FIGURE 7.24** Fourth-order symlets: (a)–(b) decomposition filters; (c)–(d) reconstruction filters; (e) the one-dimensional wavelet; (f) the one-dimensional scaling function; and (g) one of three two-dimensional wavelets, $\psi^{H}(x, y)$.

## Continuous Wavelet transform

Fig. 7.24 (Con't)

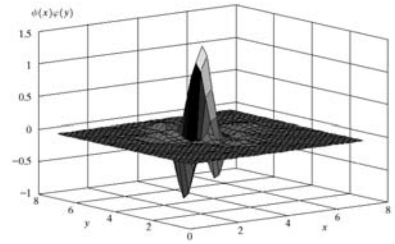

## Wavelet-based edge detection

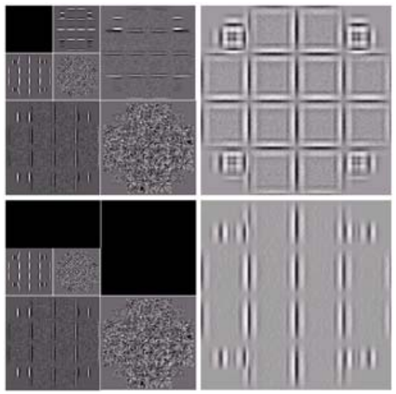

a b
c d

**FIGURE 7.25** Modifying a DWT for edge detection: (a) and (c) two-scale decompositions with selected coefficients deleted; (b) and (d) the corresponding reconstructions.

## Wavelet-based denoising

In the background, corrupted with a form of additive or multiplicative white noise.
The general wavelet-based procedure for denoising :

1. Choose a wavelet and number of levels or scales, P for the decomposition, compute FWT
2. Threshold the detail coefficients: Select and apply a threshold to the detail coefficients from scales J - 1 to J - P. This can be accomplished by hard threshholding or by soft thresholding. Soft thresholding eliminates the discontinuity at the threshold.
3. Perform a wavelet reconstruction based on the original approximation coefficients at level J - P and the modified detail coefficients for levels J - 1 to J - P .

Figure 7.26(b) : the result of performing these operations with P = 2 and a global threshold. Note the reduction in noise and corresponding loss of quality at the image edges.
Fig. 7.26(c) : the loss of edge detail is greatly reduced, which was generated by zeroing the highest-resolution detail coefficients. Most noises are gone with slightly disturbed edges.
Fig. 7.26(e) : a similar set of images involving all detail coefficients. That is, the details at both levels of the decomposition have been zeroed.

## Thresholding

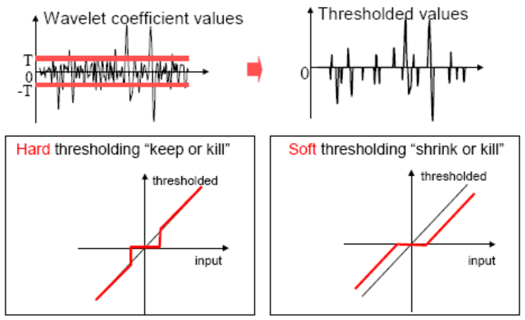


## Wavelet-based denoising

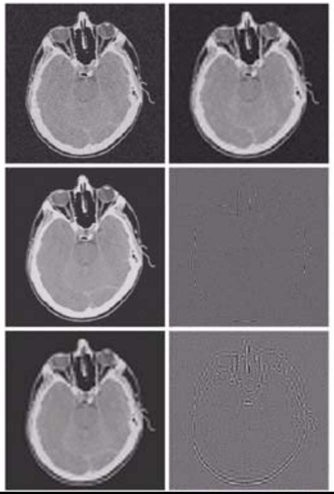

a b
c d
e f

**FIGURE 7.26** Modifying a DWT for noise removal: (a) a noisy MRI of a human head; (b), (c) and (e) various reconstructions after thresholding the detail coefficients; (d) and (f) the information removed during the reconstruction of (c) and (e). (Original image courtesy Vanderbuilt University Medical Center.)

## Wavelet Packets

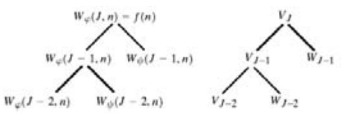


a b

**FIGURE 7.27** A coefficient (a) and analysis (b) tree for the two-scale FWT analysis bank of Fig. 7.16.

## Wavelet Packets

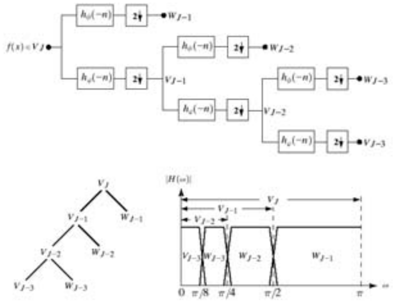


a
b c

**FIGURE 7.28** A three-scale FWT filter bank: (a) block diagram; (b) decomposition space tree; and (c) spectrum splitting characteristics.

## Wavelet Packets

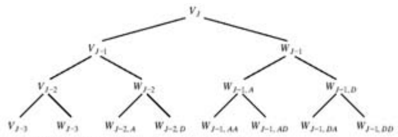

FIGURE 7.29 A three-scale wavelet packet analysis tree.

## Wavelet Packets

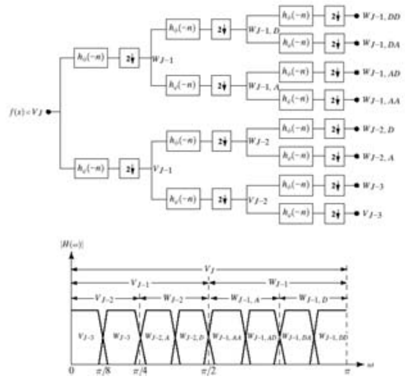

a
b
FIGURE 7.30 The (a) filter bank and (b) spectrum splitting characteristics of a three-scale full wavelet packet analysis tree.

## Wavelet Packets

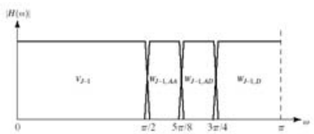

FIGURE 7.31 The spectrum of the decomposition in Eq. (7.6-5).

## Wavelet Packets

a b
FIGURE 7.32 The first decomposition of a two-dimensional FWT: (a) the spectrum and (b) the subspace analysis tree.

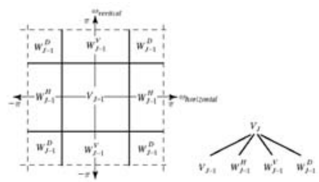

## Wavelet Packets

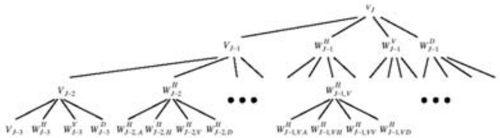

**FIGURE 7.33** A three-scale, full wavelet packet decomposition tree. Only a portion of the tree is provided.

## Wavelet Packets

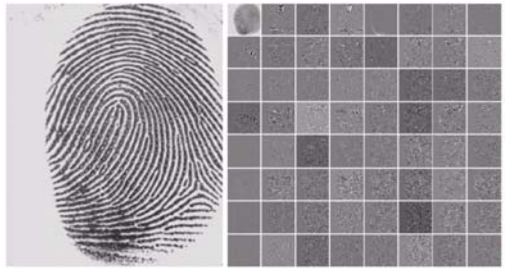

a b

**FIGURE 7.34** (a) A scanned fingerprint and (b) its three-scale, full wavelet packet decomposition. (Original image courtesy of the National Institute of Standards and Technology.)

## Wavelet Packets

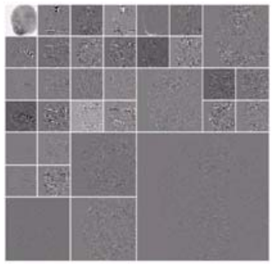

**FIGURE 7.35** An optimal wavelet packet decomposition for the fingerprint of Fig. 7.34(a).

## Wavelet Packets

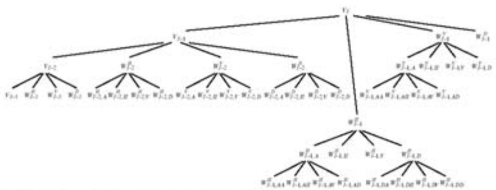

**FIGURE 7.36** The optimal wavelet packet analysis tree for the decomposition in Fig. 7.35.

## Wavelet Packets

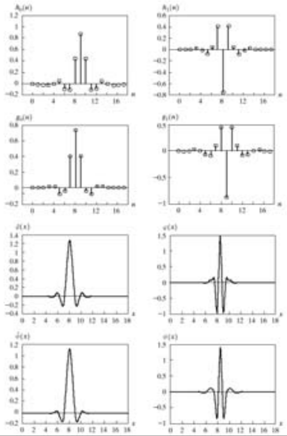

a b
c d
e f
g h

**FIGURE 7.37** A member of the Cohen-Daubechies-Feauveau biorthogonal wavelet family: (a) and (b) decomposition filter coefficients; (c) and (d) reconstruction filter coefficients; (e)–(h) dual wavelet and scaling functions.